Determination of the compound nucleus survival probability P_{surv} for various "hot" fusion reactions based on the dynamical cluster-decay model

Sahila Chopra, Arshdeep Kaur, and Raj K. Gupta
Department of Physics, Panjab University, Chandigarh 160014, India
(Received 30 December 2014; revised manuscript received 9 February 2015; published 23 March 2015)

After a successful attempt to define and determine recently the compound nucleus (CN) fusion/ formation probability P_{CN} within the dynamical cluster-decay model (DCM), we introduce and estimate here for the first time the survival probability P_{surv} of CN against fission, again within the DCM. Calculated as the dynamical fragmentation process, P_{surv} is defined as the ratio of the evaporation residue (ER) cross section σ_{ER} and the sum of σ_{ER} and fusion-fission (ff) cross section σ_{ff}, the CN formation cross section σ_{CN}, where each contributing fragmentation cross section is determined in terms of its formation and barrier penetration probabilities P_0 and P. In DCM, the deformations up to hexadecapole and "compact" orientations for both in-plane (coplanar) and out-of-plane (noncoplanar) configurations are allowed. Some 16 "hot" fusion reactions, forming a CN of mass number $A_{CN} \sim 100$ to superheavy nuclei, are analyzed for various different nuclear interaction potentials, and the variation of P_{surv} on CN excitation energy E^*, fissility parameter χ, CN mass A_{CN}, and Coulomb parameter Z_1Z_2 is investigated. Interesting results are that three groups, namely, weakly fissioning, radioactive, and strongly fissioning superheavy nuclei, are identified with P_{surv}, respectively, ~ 1, $\sim 10^{-6}$, and $\sim 10^{-10}$. For the weakly fissioning group ($100 < A_{CN} \lesssim 200$), independent of the interaction potential, different isotopes and for coplanar or noncoplanar collisions, P_{surv} decreases from one to zero as E^* increases, whereas, independent of entrance channel effects, the same is surprisingly the reverse for the radioactive group ($A_{CN} \sim 200$–250), i.e., P_{surv} increases with the increase of E^*. This is shown to be so due to the different relative magnitudes of σ_{ER} and σ_{ff} and their variations with E^* in the two cases. For the superheavy nuclei also P_{surv} is a decreasing function of E^*. Furthermore, of particular interest are the cases of ^{105}Ag*, isotopes of Pt*, and ^{213,215,217}Fr* nuclei — for ^{105}Ag*, whereas the P_{CN} belongs to the strongly fissioning superheavy group, P_{surv} belongs to weakly fissioning nuclei; for Pt* isotopes, the inverse of all the compound systems studied, both P_{CN} and P_{surv} decrease with the increase of E^*; for ^{213,215,217}Fr* nuclei, though fissility χ is nearly the same, P_{surv} for ^{213,217}Fr* is of the same order as for weakly fissioning nuclei, but that for ^{215}Fr* is of the order of radioactive nuclei. Apparently, further calculations are called for.

DOI: 10.1103/PhysRevC.91.034613 PACS number(s): 25.70.Gh, 25.70.Jj, 25.60.Pj, 24.60.Dr

I. INTRODUCTION

In a very recent work [1,2], we determined the compound nucleus (CN) fusion/formation probability P_{CN} within the dynamical cluster decay model (DCM), defined as

$$P_{CN} = \frac{\sigma_{CN}}{\sigma_{fusion}} = 1 - \frac{\sigma_{nCN}}{\sigma_{fusion}}, \quad (1)$$

where the (total) fusion cross section $\sigma_{fusion} = \sigma_{CN} + \sigma_{nCN}$ with σ_{CN} as the CN formation cross section, given as the sum of evaporation residue (ER) and fusion-fission (ff) cross sections ($\sigma_{CN} = \sigma_{ER} + \sigma_{ff}$), and σ_{nCN} as the noncompound nucleus (nCN) cross section. Figure 1 in Ref. [1], illustrates schematically the various components of CN decay/fusion cross section, also called the CN production cross section, or simply the (total) fusion cross section σ_{fusion} if the nCN component is included.

Another quantity of interest in heavy ion reactions, not fully understood, is the CN survival probability P_{surv}, introduced to account for the emission of light particles (LPs) or neutrons with respect to the fusion-fission process. In other words, P_{surv} is the probability that the fused system will de-excite by emission of neutrons or LPs (equivalently, the evaporation residue ER) rather than fission, thereby defined as

$$P_{surv} = \frac{\sigma_{ER}}{\sigma_{CN}}, \quad (2)$$

where $\sigma_{CN} = \sigma_{ER} + \sigma_{ff}$, as defined above. Apparently, for a fissionless decay, $P_{surv} = 1$, i.e., the CN decays via neutrons or LPs emission alone. On the other hand, if only fission takes place, then $P_{surv} = 0$, implying that no neutron's (or LPs) emission occur and there is a complete instability against fission. It is evident from above that P_{CN} takes care of the nCN effects, and P_{surv} looks after the ff process. Then, from Eqs. (1) and (2), the evaporation residue cross section σ_{ER}, with the effects of both ff and nCN processes included, can be written as

$$\sigma_{ER} = \sigma_{CN} P_{surv} = \sigma_{fusion} P_{CN} P_{surv}, \quad (3)$$

which gives the CN decay cross section σ_{CN} if $P_{surv} = 1$ (i.e., $\sigma_{ff} = 0$), and the total fusion cross section σ_{fusion} if both $P_{CN} = 1$ and $P_{surv} = 1$ (i.e., $\sigma_{nCN} = 0$ as well as $\sigma_{ff} = 0$, respectively). Apparently, the survival probability P_{surv} of the CN, in its de-excitation against fission, is a more crucial factor for producing heavy and superheavy nuclei. However, the P_{CN} also becomes equally important, if nCN effects, like the quasifission (qf), deep-inelastic collisions/orbiting (DIC), incomplete fusion (ICF) or pre-equilibrium decay, also comes in to play.

In statistical models, the survival probability is formally written as $P_{\mathrm{surv}} = \Pi_{i=1}^{x}\frac{\Gamma_n^i}{\Gamma_n^i+\Gamma_{\mathrm{fiss}}^i}$ for each successive emission of x neutrons and the fission, with respective widths Γ_n^i and Γ_{fiss}^i, and can be estimated empirically by using experimental data, as well as derived theoretically by using the classical formalism of Vandenbosch and Huizenga [3] based on the standard Fermi-gas level density formula with different expressions for the level density parameter [4,5], and Kramers [6] dissipation factor included or not included, mainly used for superheavy nuclei formed in "cold" fusion reactions. As an alternative prescription, here we define P_{surv}, for the first time, on the basis of the dynamical cluster-decay model (DCM) of Gupta and collaborators [7–26] for "hot" fusion reactions, whose first report was made at a recent conference [27]. Here, we extend this work to a larger number of reactions (about 16) having nonzero σ_{ff} component, to more than one nuclear interaction, and to a larger number of variables on which the P_{surv} could depend. Note that, in DCM, the CN fusion cross section σ_{CN} depends not only on "barrier penetrability" P, but also on fragment preformation factor P_0. It may be recalled that different combinations of the decay processes (ER, ff, and nCN), or a single one of them as the dominant constituent, come in to play in different mass regions of compound nuclei.

In this paper, we consider an application of Eq. (2) to a set of some 16 reactions with different target-projectile combinations leading to different compound nuclei. The calculations are made on the basis of systematic analysis of experimental data using the DCM [13–25], which include the possible role of deformations up to hexadecapole deformations (β_2, β_3, β_4), with compact orientations $\theta_{ci}, i = 1,2$ [28], or up to only quadrupole deformation (β_{2i}), with "optimum" orientations $\theta_i^{\mathrm{opt.}}$ [29], of "hot" fusion process, for both the cases of coplanar (azimuthal angle $\Phi = 0^\circ$) and noncoplanar ($\Phi \neq 0^\circ$) nuclei, using different nuclear interactions. The model is quite general, describing completely both the ER and ff processes with in a single parameter description, the neck length parameter ΔR, which, for a given temperature, is allowed to take different values for different processes. The aim of this work is to study within the DCM, the effect of various reaction characteristics, such as the CN excitation energy E^*, fissility parameter χ $(=(Z^2/A)/48)$, CN mass number A_{CN} and the Coulomb interaction parameter Z_1Z_2, on P_{surv}.

The organization of the paper is as follows. Section II gives a brief description of the dynamical cluster-decay model (DCM). The calculations for survival probability P_{surv}, based on DCM, are given in Sec. III. Finally, a summary and conclusions are presented in Sec. IV.

II. DYNAMICAL CLUSTER-DECAY MODEL

The DCM, based on the well-known quantum mechanical fragmentation theory (QMFT) of fission, heavy ion reactions, and exotic cluster radioactivity (see, e.g., Refs. [7,29]), is worked out in terms of the collective coordinates of mass (and charge) asymmetries $\eta = (A_1 - A_2)/(A_1 + A_2)$ (and $\eta_Z = (Z_1 - Z_2)/(Z_1 + Z_2)$), and relative separation R, with multipole deformations $\beta_{\lambda i}$ ($\lambda = 2,3,4$; $i = 1,2$, referring to heavy and light fragments, respectively), and orientations θ_i, Φ. In terms of these coordinates, for ℓ partial waves, we define the compound nucleus decay/formation cross section for each fragmentation (A_1, A_2) as

$$\sigma_{(A_1,A_2)} = \frac{\pi}{k^2}\sum_{\ell=0}^{\ell_{\max}}(2\ell+1)P_0P; \quad k = \sqrt{\frac{2\mu E_{\mathrm{c.m.}}}{\hbar^2}}, \tag{4}$$

where P_0 is preformation probability, referring to η motion at a fixed R value and P, the penetrability, to R motion for each η value, both dependent on angular momentum ℓ and temperature T. μ is reduced mass with m as the nucleon mass. $\ell_{\max}$ is the maximum angular momentum, defined for light particle evaporation residue cross section $\sigma_{\mathrm{ER}} \to 0$. The temperature T (in MeV) is related to CN excitation energy E^* $(=E_{\mathrm{c.m.}} + Q_{\mathrm{in}}$, with $E_{\mathrm{c.m.}}$ as the entrance channel center-of-mass energy and Q_{in}, the corresponding Q value) as

$$E^* = (A/a)T^2 - T,$$

with the level density parameter $a = 9$–11, depending on mass A of the CN.

In QMFT, in general, the η and R motions are coupled, but, as justified in Refs. [30–33], in the definition of Eq. (4) above, these are apparently taken as decoupled. The stationary Schrödinger equation for the coupled η and R coordinates (with the η_Z coordinate minimized, hence kept fixed), is given by

$$H(\eta,R)\psi(\eta,R) = E\psi(\eta,R) \tag{5}$$

with the Hamiltonian constructed as

$$\begin{aligned} H(\eta,R) = {} & E(\eta) + E(R) + E(\eta,R) \\ & + V(\eta) + V(R) + V(\eta,R), \end{aligned} \tag{6}$$

where E refers to the kinetic energy (expressed in terms of mass parameters B_{ij}; $i,j = R,\eta$ [34–36]) and $V(\eta,R,T)$, the T-dependent collective potential energy, calculated as per the Strutinsky renormalization procedure ($B = V_{\mathrm{LDM}} + \delta U$), using the T-dependent liquid drop model energy $V_{\mathrm{LDM}}(T)$ of Davidson *et al.* [37] with its constants at $T = 0$ refitted [9,10,13] to give the experimental binding energies of Audi *et al.* [38], and the "empirical" shell corrections δU of Myers and Swiatecki [39] for spherical nuclei, also made T dependent to vanish exponentially, added to T-dependent nuclear proximity V_P, Coulomb V_C, and ℓ-dependent potential V_ℓ for deformed, oriented nuclei. In $V_\ell(T)$ $(=\frac{\hbar^2\ell(\ell+1)}{2I(T)})$, the moment of inertia I is either in complete sticking limit $I = I_S(T) = \mu R^2 + \frac{2}{5}A_1 m R_1^2(\alpha_1,T) + \frac{2}{5}A_2 m R_2^2(\alpha_2,T)$ or, as for experiments, in the nonsticking limit $I = I_{\mathrm{NS}} = \mu R^2$. The angles α_i, $i = 1,2$, used to define the radius vectors R_i of deformed nuclei [see Eq. (9) below], are measured in the clockwise direction from the symmetry axis. We find that the use of sticking limit I_S is more appropriate for the proximity potential (nuclear surfaces $\leqslant 2$ fm apart), which evidently has consequences for the limiting $\ell_{\max}$ value to be much larger. For nuclear collisions, the use of the larger $\ell_{\max}$ value due to the relatively larger magnitude of I_S is shown [13,16] to result in the reduction of the nuclear surface separation distance ΔR [defined in Eq. (8) below], and vice versa for $I_{\rm NS}$. For V_P, we use the pocket formula of Blocki *et al.* [40] and various Skyrme forces (SIII and GSkI) in Skyrme energy density formalism (SEDF) [41–43]. For the kinetic energy part, the mass parameters $B_{\eta\eta}$ used are the smooth classical hydrodynamical masses [34] though, in principle, the shell corrected masses, like the cranking masses which depend on the underlying shell model basis [35,36], should be used. In QMFT, however, the shell effects in B_{ij} do not play much of a role [30,31].

To implement the decoupled approximation in Eq. (5), (i) the kinetic energy coupling term $E(\eta,R)$ ($\propto\frac{\partial^2}{\partial\eta\partial R}$) is neglected since the coupled cranking masses $B_{R\eta}$ and $B_{R\eta_Z}$ [35,36] are very small [30,31], such that the relations $B_{R\eta}\ll(B_{RR}B_{\eta\eta})^{\frac{1}{2}}$ and $B_{R\eta_Z}\ll(B_{RR}B_{\eta_Z\eta_Z})^{\frac{1}{2}}$ hold good; (ii) the coupling term of the potential $V(\eta,R)$ is shown to be small [32,33], at least for fission charge distributions [32] and α-particle transfer resonances [33]. Then the Hamiltonian (6) for each ℓ value, on using the Pauli-Podolsky prescription [44], takes the following form

$$H=-\frac{\hbar^2}{2\sqrt{B_{\eta\eta}}}\frac{\partial}{\partial\eta}\frac{1}{\sqrt{B_{\eta\eta}}}\frac{\partial}{\partial\eta}-\frac{\hbar^2}{2\sqrt{B_{RR}}}\frac{\partial}{\partial R}\frac{1}{\sqrt{B_{RR}}}\frac{\partial}{\partial R}+V(\eta)+V(R), \tag{7}$$

and then the Schrödinger equation (5) becomes separable in the two coordinates η and R, whose solutions $|\psi(\eta)|^2$ and $|\psi(R)|^2$ give, respectively, the probabilities P_0 and P of Eq. (4). The $P_0(A_i)$ is obtained at a fixed $R=R_a$, the first turning point(s) of the penetration path(s) for different ℓ values, and the penetrability P, instead of solving the radial Schrödinger equation in R, is given by the WKB integral, which is solved analytically [45,46]. For more details, see Ref. [1].

For R_a, in the decay of a hot CN, we use the postulate [8–10]

$$\begin{aligned}R_a(T)&=R_1(\alpha_1,T)+R_2(\alpha_2,T)+\Delta R(\eta,T),\\&=R_t(\alpha,\eta,T)+\Delta R(\eta,T),\end{aligned} \tag{8}$$

with radius vectors

$$R_i(\alpha_i,T)=R_{0i}(T)\left[1+\sum_\lambda\beta_{\lambda i}Y_\lambda^{(0)}(\alpha_i)\right] \tag{9}$$

having temperature-dependent nuclear radii $R_{0i}(T)$ for the equivalent spherical nuclei [47]

$$R_{0i}=\left[1.28A_i^{1/3}-0.76+0.8A_i^{-1/3}\right](1+0.0007T^2). \tag{10}$$

Thus, R_a introduces a T-dependent parameter $\Delta R(T)$, the neck-length parameter, which assimilates the deformation and neck formation effects between two nuclei [48–50]. As the ℓ-value increases, the potential $V(R_a,\ell)$ increases, and hence R_a acts like a parameter through $\Delta R(\eta,T)$. We define R_a same for all ℓ values since we do not know how to add the ℓ effects in binding energies. Furthermore, the parameter ΔR introduces in DCM an in-built property of "barrier lowering" since, for a best fit to the data, it allows us to relate in a simple way the $V(R_a,\ell)$ to the top of the barrier $V_B(\ell)$ for each ℓ, by defining their difference $\Delta V_B(\ell)$ as the effective "lowering of the barrier"

$$\Delta V_B(\ell)=V(R_a,\ell)-V_B(\ell). \tag{11}$$

Note, ΔV_B for each ℓ is defined as a negative quantity since the actually used barrier is effectively lowered [7,14].

Noting that the DCM equation (4) is defined in terms of the exit/decay channels alone, i.e., both the formation P_0 and then the emission via barrier penetration P are calculated only for decay channels (A_1, A_2), it follows from Eq. (4) that

$$\sigma_{\rm ER}=\sum_{A_2=1}^{4\,\rm or\,5}\sigma_{(A_1,A_2)}\quad\text{or}\quad=\sum_{x=1}^{4\,\rm or\,5}\sigma_{xn}, \tag{12}$$

and

$$\sigma_{\rm ff}=2\sum_{A_2=5\,\rm or\,6}^{A/2}\sigma_{(A_1,A_2)}, \tag{13}$$

giving $\sigma_{\rm CN}=\sigma_{\rm ER}+\sigma_{\rm ff}$. Equation (13) is also applicable to intermediate mass fragments (IMFs) cross section $\sigma_{\rm IMFs}$, with the sum taken up to the maximum measured value of A_2 and without the multiplying factor of 2. The same formula (4) is also applied to the nCN decay process, calculated here as the quasifission (qf) decay channel where $P_0=1$ since for qf the incoming target and projectile nuclei can be considered to have not yet lost their identity, and then P is calculated for the *incoming channel* $\eta_{\rm ic}$, as

$$\sigma_{\rm nCN}=\frac{\pi}{k^2}\sum_{\ell=0}^{\ell_{\max}}(2\ell+1)P_{\eta_{\rm ic}}, \tag{14}$$

known in the literature as the (ℓ summed) extended-Wong model formula [51]. Thus, the DCM predicts not only the total fusion cross section, the sum of the constituents ER, ff, and nCN, but also the cross sections of the constituents themselves.

III. CALCULATIONS AND RESULTS

In this section, we present the results of our calculations for the CN survival probability $P_{\rm surv}$, based on the calculations made on the DCM for the chosen 16 reactions, giving different compound nuclei, for all possible decay processes at different center-of-mass energies $E_{\rm c.m.}$. The chosen reactions, their characteristic properties, and the calculated $P_{\rm surv}$ and $P_{\rm CN}$ on the DCM, including the $P_{\rm CN}$ from Ref. [1] for the earlier studied 12 cases, are listed in Table I. The chosen reactions span the excited compound systems from mass number $A\sim100$ to superheavy nuclei, i.e., from all the three regions of stable, radioactive, and superheavy mass. Note that the reactions involved are all "hot" fusion reactions. Best fits to data were made for $\sigma_{\rm ER}$, $\sigma_{\rm ff}$ (or $\sigma_{\rm IMFs}$), and the measured or empirically obtained $\sigma_{\rm qf}$ (or $\sigma_{\rm nCN}$ calculated as the qf process). The empirical nCN component is estimated as

$$\sigma_{\rm nCN}^{\rm empirical}=\sigma_{\rm fusion}^{\rm Expt.}-\sigma_{\rm fusion}^{\rm Cal.}. \tag{15}$$

The possible effect of using different nuclear proximity potentials, e.g., the pocket formula of Blocki *et al.* or nuclear potentials due to different Skyrme forces in Skyrme energy density formalism (SEDF), and different azimuthal angles Φ, i.e., for coplanar ($\Phi=0^\circ$) and noncoplanar ($\Phi\neq0^\circ$)

TABLE I. Characteristic properties of the 16 chosen reactions investigated on the DCM, using the pocket formula of Blocki *et al.* [40] and Skyrme energy density formalism (SEDF) [19,20], for the compound nucleus excitation energy range $E^* = 22.92$–84.2 MeV, arranged per three groups of P_{surv} decreasing (having a large or small value) or increasing (having a small value) with E^*. The large P_{surv} refers to small σ_{ff} and vice versa.

Reactions	Φ (deg.)	Z	A_{CN}	E^* (MeV)	Z_1Z_2	χ	P_{CN} Ref. [1]	P_{surv}	Ref. No.
				Blocki *et al.* Pocket formula					
$^{64}Ni + ^{100}Mo \to ^{164}Yb^*$	0	70	164	30.6–66.5	1176	0.622	0.62–0.94	0.99–0.44	[14]
$^{64}Ni + ^{100}Mo \to ^{164}Yb^*$	$\neq 0$	70	164	30.6–66.5	1176	0.622	0.784–1	0.995–0.515	[19]
$^{48}Ca + ^{154}Sm \to ^{202}Pb^*$	0	82	202	44.5–65.3	1240	0.693	0.77–0.89	0.822–0.243	[15]
$^{12}C + ^{93}Nb \to ^{105}Ag^*$	0	47	105	40.95–54.06	246	0.438	0.13–0.25	0.421–0.037	[21]
$^{64}Ni + ^{112}Sn \to ^{176}Pt^*$	0	78	176	22.92–61.42	1400	0.72	1–0.927	0.899–0.108	[18]
$^{64}Ni + ^{118}Sn \to ^{182}Pt^*$	0	78	182	33.215–70.465	1400	0.696	1–0.91	0.917–0.185	[18]
$^{64}Ni + ^{124}Sn \to ^{188}Pt^*$	0	78	188	44.337–77.487	1400	0.674	1–0.543	0.985–0.564	[18]
$^{132}Sn + ^{64}Ni \to ^{196}Pt^*$	0	78	196	54.498–84.2	1400	0.646	1–0.696	0.852–0.466	[18]
$^{19}F + ^{198}Pt \to ^{217}Fr^*$	0	87	217	43.479–69.650	702	0.727	1	0.644–0.267	[24,25]
$^{19}F + ^{194}Pt \to ^{213}Fr^*$	0	87	213	47.397–61.059	702	0.740	1	0.471–0.079	[24,25]
$^{32}S + ^{92}Mo \to ^{124}Ce^*$	0	58	124	46.5	672	0.565	0.88	0.58	[22]
$^{48}Ca + ^{238}U \to ^{286}Cn^*$	0	112	286	33.1–40.78	1840	0.91	0.005–0.2	2.20×10^{-10}–2.10×10^{-11}	[16]
$^{244}Pu + ^{48}Ca \to ^{292}Fl^*$	0	114	292	35.51–36.73	1880	0.93	0.113–0.14	3.34×10^{-10}–2.72×10^{-10}	[17]
$^{14}N + ^{232}U \to ^{246}Bk^*$	0	97	246	43–60.9	630	0.796	0.978–1	2.9×10^{-7}–4.2×10^{-5}	[13]
$^{11}B + ^{235}U \to ^{246}Bk^*$	0	97	246	34.3–55.9	460	0.796	1–0.78	4.9×10^{-8}–8.0×10^{-5}	[13]
$^{11}B + ^{204}Pb \to ^{215}Fr^*$	0	87	215	31.21–43.48	410	0.733	1	7.07×10^{-7}–3.66×10^{-5}	[23]
$^{18}O + ^{197}Au \to ^{215}Fr^*$	0	87	215	39.10–56.57	632	0.733	1	9.09×10^{-7}–1.46×10^{-4}	[23]
				SEDF(SIII/ GSkI)					
$^{132}Sn + ^{64}Ni \to ^{196}Pt^*$	0	78	196	56.2–84.2	1400	0.646	1–0.41	0.644–0.378	[20]
$^{64}Ni + ^{100}Mo \to ^{164}Yb^*$	0	70	164	30.6–66.5	1176	0.622	0.94–1	0.495–0.999	[19]

nuclei, are also investigated. Except in the case of the $^{48}Ca + ^{154}Sm$ reaction (where only spherical nuclei are considered), deformed, oriented configurations are allowed in all other above-stated works carried out on the DCM. Like for P_{CN} in Ref. [1], it is of interest to study the variation of P_{surv} with the CN excitation energy E^*, the CN charge Z (or mass A) number, the fissility parameter χ $(=(Z^2/A)/48)$, and the reaction entrance channels in terms of quantities such as the Coulomb interaction parameter Z_1Z_2. Some of these results, based on the DCM calculations, are presented in the following.

Figure 1 shows the variation of DCM-calculated P_{surv} with CN excitation energy E^*, in Fig. 1(a) for five compound systems ($^{105}Ag^*$, $^{164}Yb^*$, $^{176}Pt^*$, $^{202}Pb^*$, and $^{217}Fr^*$) formed in reactions with coplanar ($\Phi = 0°$) nuclei, and for $^{164}Yb^*$, also for the case of noncoplanar ($\Phi \neq 0°$) nuclei; in Fig. 1(b) for the $\Phi = 0°$ case of different isotopes of Pt* and Fr* ($^{176,182,188,196}Pt^*$ and $^{213,217}Fr^*$), and in Fig. 1(c) for different Skyrme forces (SIII, SSk, and GSkI) used for the $\Phi = 0°$ case of reactions forming $^{164}Yb^*$ and $^{196}Pt^*$. Interestingly, for all the considered CN, independent of in-plane or out-of-plane orientations of nuclei, their different isotopes and the choice of different nuclear interaction potentials, the survival probability P_{surv} of CN against fission decreases with increasing E^*, going from 1 to 0. This essentially means that the fission becomes more prominent, i.e., the fusion-fission component σ_{ff} increases with the increase of E^* [refer to σ_{ff} in Fig. 4(b) below, for $^{202}Pb^*$; the same is true of other compound systems in Fig. 1. Another point to note in Fig. 4(b) is that σ_{ER} and σ_{ff} are comparable at all E^*'s, leading to the decrease of P_{surv} with the increase of E^*]. In other words, the stability of these nuclei against fission decreases with the increase of E^*. Note that none of these CN are radioactive, i.e., this is a group of weakly fissioning nuclei, and that $^{213,217}Fr^*$ belong to this group. Furthermore, Fig. 1(b) shows that $^{213}Fr^*$ is more fissile (lower P_{surv}) as compared to $^{217}Fr^*$, as expected [24]. Another interesting point to note is that, except for Pt* isotopes, in all other cases, the CN formation probability P_{CN} increases with E^* (see Fig. 4 in Ref. [1]), a behavior reverse of P_{surv} with E^*. For Pt* isotopes, however, both P_{CN} and P_{surv} decrease with the increase of E^*, which should have interesting consequences for σ_{ER} [refer to Eq. (3)].

Similarly as above, for DCM-studied superheavy nuclei $^{286}_{112}Cn^*$ [16] and $^{292}_{114}Fl^*$ [17], considered here, we know from experiments that the fusion-fission component σ_{ff} increases as E^* increases (see, Fig. 4 in Ref. [16] or Fig. 5 in Ref. [17]), and hence P_{surv} would decrease with the increase of E^*, as is depicted to be the case in Fig. 2. Since these are strongly fissioning nuclei ($\sigma_{ff} \sim$ mb relative to $\sigma_{ER} \sim$ pb [16,17]), P_{surv} is very small $\sim 10^{-10}$.[1] Note that the CN formation probability P_{CN} for these nuclei is also small ($\sim$0.1–0.2), as is the case for $^{105}Ag^*$ (see, Fig. 4 in Ref. [1]) whose P_{surv} is, however, large ($\sim$0.42–0.04), as discussed in the last paragraph above [Fig. 1(a)]. Thus, $^{105}Ag^*$ actually belongs to weakly fissioning

[1]There is an error of order in Fig. 1(b) of Ref. [27]. It should be 10^{-10} instead of 10^{-4}.

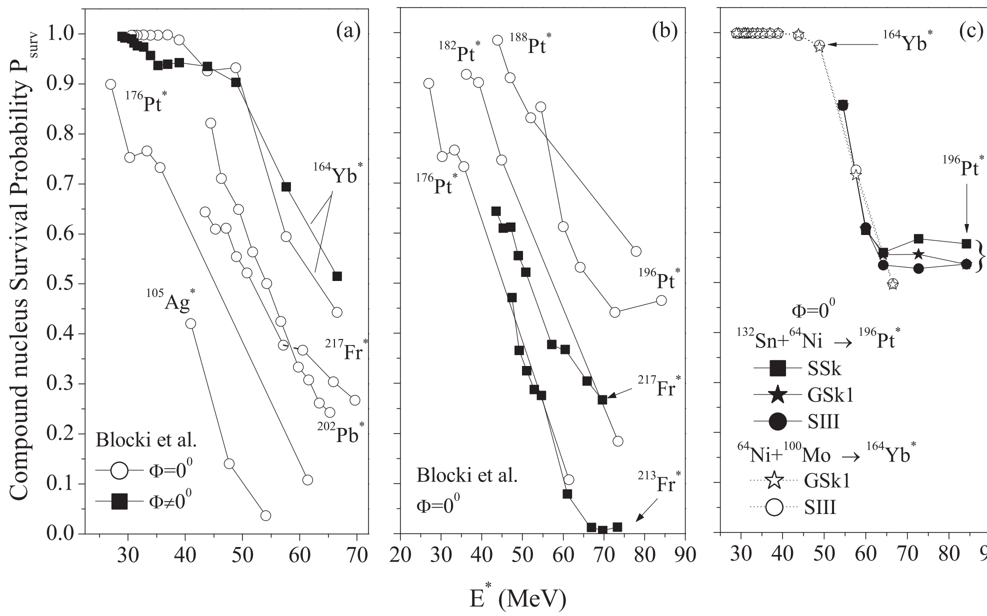

FIG. 1. The DCM-calculated P_{surv} as a function of CN excitation energy E^*, using for nuclear proximity potential, the Blocki *et al.* [40] pocket formula, (a) for coplanar ($\Phi = 0^\circ$) case of different CN, compared to the noncoplanar ($\Phi \neq 0^\circ$) case of ^{164}Yb*, (b) for different isotopes ^{176,182,188,196}Pt* and ^{213,217}Fr*, and (c) $\Phi = 0^\circ$ case of SEDF, using SIII, SSk, and GSkI forces in ^{196}Pt* [20] and ^{164}Yb* [19].

nuclei, though its P_{CN} is of the same order as for strongly fissioning superheavy nuclei.

Next, Fig. 3 shows the results of our DCM-calculated P_{surv} as a function of E^* for two radioactive nuclei (^{246}Bk* [13] and ^{215}Fr* [23]), each formed via two different incoming channels. We notice that, independent of the entrance channel, instead of decreasing, i.e., contrary to Figs. 1 and 2, the P_{surv} increases with increasing E^* for both the compound systems. This happens because of the strongly differing relative magnitudes of σ_{ER} and σ_{ff} and their variations with E^*, in the two cases (radioactive and weakly fissioning nuclei). This is illustrated

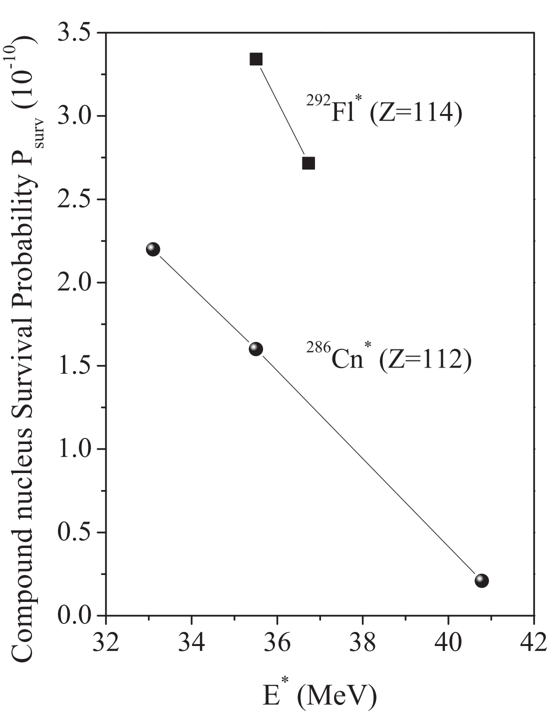

FIG. 2. Same as for Fig. 1(a) ($\Phi = 0^\circ$ case), but for superheavy nuclei ^{286}Cn* and ^{292}Fl*.

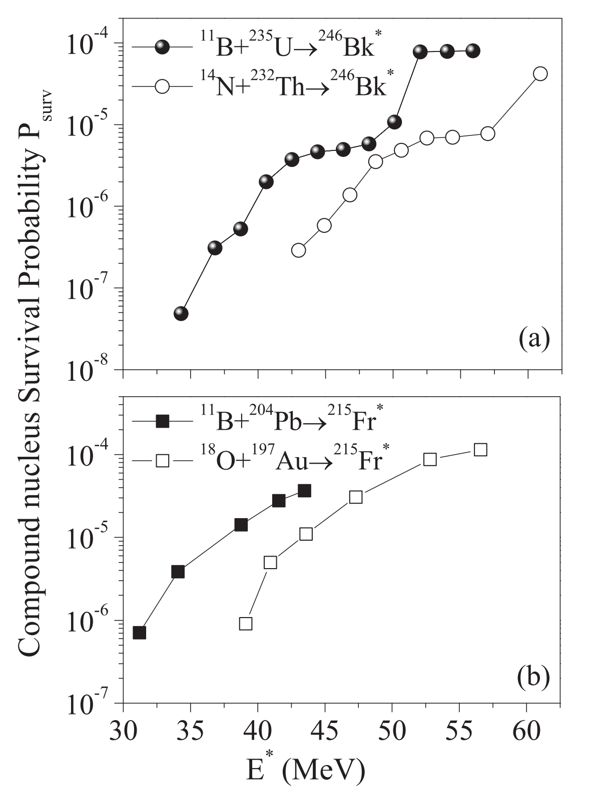

FIG. 3. Same as Fig. 1(a) ($\Phi = 0^\circ$ case), but for (a) ^{246}Bk* and (b) ^{215}Fr*.

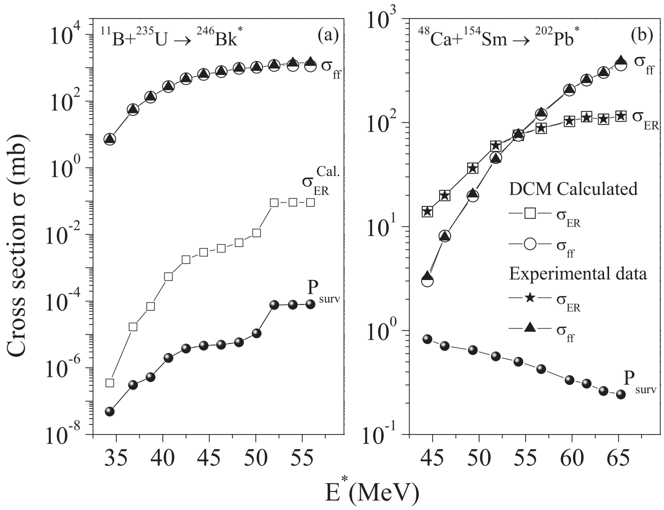

FIG. 4. The DCM-calculated $\sigma_{\rm ER}$ and $\sigma_{\rm ff}$ plotted as a function of E^* for the radioactive ^{246}Bk* and the weakly fissioning ^{202}Pb* nuclei, compared to the experimental data. For ^{246}Bk*, the experimental data are only for $\sigma_{\rm fission}$ ($\equiv\sigma_{\rm ff}\equiv\sigma_{\rm fusion}$), and $\sigma_{\rm ER}$ is for the DCM-predicted numbers. $P_{\rm surv}$ is also plotted in each case.

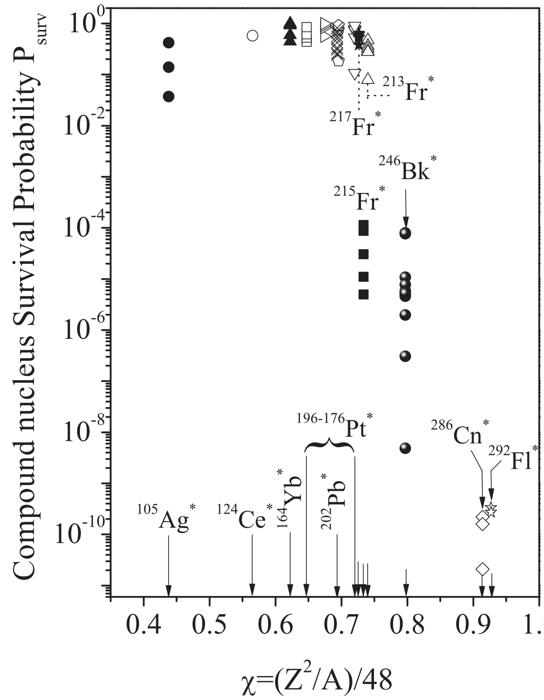

FIG. 5. Variation of $P_{\rm surv}$ with the fissility parameter χ for all the reactions under consideration.

in Fig. 4 where the variations of DCM-calculated $P_{\rm surv}$, $\sigma_{\rm ER}$, and $\sigma_{\rm ff}$ with E^* are plotted for the radioactive ^{246}Bk* and the weakly fissioning ^{202}Pb* nuclei, compared to the available experimental data. The DCM-calculated cross sections fit the experimental data very nicely. We further notice in Fig. 4(b) that the $\sigma_{\rm ER}$ and $\sigma_{\rm ff}$ are nearly of the similar magnitudes in the case of weakly fissioning ^{202}Pb*, whereas in Fig. 4(a) for the radioactive ^{246}Bk* nucleus, relative to $\sigma_{\rm ff}$, the $\sigma_{\rm ER}$ is negligibly small, such that the $P_{\rm surv}$ is small $\sim 10^{-8}$–10^{-4} and, very similar to the variation of $\sigma_{\rm ER}$, increases with increasing E^*. Note that, in the case of ^{246}Bk*, the $\sigma_{\rm ER}$ is not a measured quantity, and hence $P_{\rm surv}$ should be zero. However, in Fig. 4(a), only the DCM predicted $\sigma_{\rm ER}$ is plotted, and in both ^{202}Pb* and ^{246}Bk* nuclei, the $\sigma_{\rm ER}$ and $\sigma_{\rm ff}$ increase with increasing E^*. The same is true of other weakly fissioning and radioactive nuclei considered in Figs. 1 and 3, respectively. Another interesting result of Fig. 3 is that ^{215}Fr* behaves similarly to strongly fissioning radioactive ^{246}Bk*, whereas ^{213,217}Fr* are shown above to belong to the weakly fissioning group of nuclei. Note that ^{215}Fr in the ground state is known to be the least stable isotope of the 34 known isotopes of Fr ($^{199-232}$Fr).

Figure 5 shows the variation of $P_{\rm surv}$ with fissility parameter $\chi=(Z^2/A)/48$ for all the 16 compound systems, studied at various excitation energies E^*. We notice that $P_{\rm surv}$ approaches unity for the ten systems belonging to lower fissility or the weakly fissioning region, forming two groups: (i) $P_{\rm surv}\sim$ 0.822–0.995 for ^{164}Yb*, ^{176,182,188,192}Pt* and ^{202}Pb* with χ lying between 0.622–0.72, and (ii) for the other four compound systems ^{105}Ag*, ^{124}Ce* and ^{217,213}Fr*, $P_{\rm surv}\sim$ 0.421–0.644 at $\chi=0.44, 0.565, 0.727$, and 0.740. Interestingly, though the χ value for the three ^{217,215,213}Fr* nuclei are nearly identical, ^{215}Fr* (with $\chi=0.733$) belongs to the group of strongly fissioning radioactive ^{246}Bk* with $\chi=0.796$, both having $P_{\rm surv}$ very small $\sim 10^{-8}$–10^{-4}, increasing with E^*. Note, however, that $P_{\rm surv}$ for the two superheavy systems ^{286}Cn* and ^{292}Fl* is further very small $\sim 10^{-10}$–10^{-11} at higher $\chi=0.914$ and 0.927, respectively, decreasing with E^*. Apparently, the later two groups of CN (^{215}Fr*, ^{246}Bk*, and two superheavy ^{286}Cn* and ^{292}Fl*) are least stable against fission, with the variation of $P_{\rm surv}$ with χ for superheavy nuclei, similar to that of $P_{\rm CN}$ with χ (see Fig. 7 in Ref. [1]), and that $P_{\rm surv}$ distinguishes ^{105}Ag* from the superheavy nuclei, more clearly than the $P_{\rm CN}$.

Figure 6 shows the variation of $P_{\rm surv}$ with CN mass number $A_{\rm CN}$. Three groups are evident: one of lower CN mass region $100<A_{\rm CN}\lesssim 200$ with $P_{\rm surv}\to 1$, another of $\sim$200–250 with $P_{\rm surv}\sim 10^{-8}$–10^{-4}, and the third one of superheavy nuclei with $P_{\rm surv}\sim 10^{-10}$–$10^{-11}$. Interestingly, ^{213,217}Fr* belong to the first group of weakly fissioning nuclei, and ^{215}Fr* to the second group of radioactive ^{246}Bk* with almost no entrance channel effects on $P_{\rm surv}$.

The above results are best presented in Fig. 7 where $P_{\rm surv}$ is plotted as a function of the Coulomb interaction parameter Z_1Z_2, the product of target-projectile charge numbers of the reaction forming CN. Interestingly, three clear groups are formed: (i) $P_{\rm surv}\to 1$ for the ten compound nuclei ^{105}Ag*, ^{124}Ce*, ^{164}Yb*, $^{176-196}$Pt*, ^{202}Pb*, and ^{213,217}Fr* with the Coulomb interaction parameter lying in the range $240<Z_1Z_2<1400$. (ii) $P_{\rm surv}\sim 10^{-8}$–10^{-4} for the two strongly fissioning ^{215}Fr* and ^{246}Bk* nuclei, with $410<Z_1Z_2<632$ strongly dependent on the entrance channel. Interestingly, the limiting values of the product Z_1Z_2 for one entrance channel of ^{215}Fr* is about the same as for another entrance channel of ^{246}Bk*. Noting that, compared to ^{215}Fr* and ^{246}Bk*, the Z_1Z_2 for the target-projectile combination forming ^{217,213}Fr* is much larger (compare 702 to 410 and 632), possibly traces

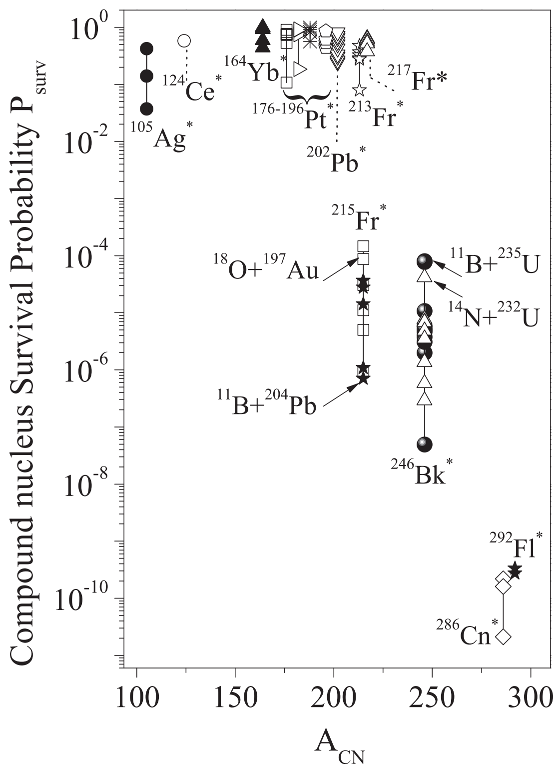

FIG. 6. Variation of P_{surv} with the compound nucleus mass number A_{CN} for all the reactions under consideration.

the reason for ^{215}Fr* to belong to ^{246}Bk* group of radioactive nuclei. (iii) The region of superheavy nuclei ^{286}Cn* and ^{292}Fl* with $Z_1Z_2 = 1840$ and 1880, respectively, having much smaller $P_{\mathrm{surv}} \sim 10^{-10}$–$10^{-11}$, apparently due to a much larger fusion-fission component. Comparing the results of group (i) with group (iii), ^{105}Ag* and superheavy nuclei belong to two limiting Z_1Z_2 values, as expected. Thus, like for P_{CN}, P_{surv} also depends strongly on Coulomb repulsion.

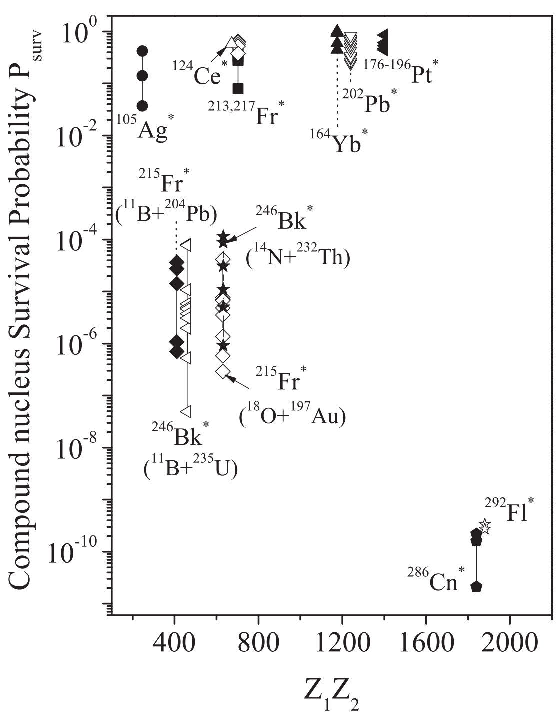

FIG. 7. Variation of P_{surv} with product Z_1Z_2 of target and projectile charge numbers.

IV. SUMMARY AND CONCLUSION

Following our earlier work on defining and estimating the CN fusion/formation probability P_{CN} on the basis of the DCM [1,2], the present work introduces and determines for the first time, on the same basis (the DCM), the probability of survival P_{surv} of CN against fission. P_{surv} ($=\sigma_{\mathrm{ER}}/\sigma_{\mathrm{CN}}$), is the ratio of the fusion evaporation residue cross section σ_{ER} to the CN formation cross section σ_{CN}, a sum of σ_{ER} and fusion-fission cross section σ_{ff}, each calculated as the dynamical fragmentation process. The contributing fragments for ER are the light particles $A_2 \leqslant 4$ or neutrons (plus the complementary heavy fragments) and for ff the near-symmetric and symmetric ($A_1 = A_2 = A/2$) fragments, including the IMFs with $5 \leqslant A_2 \leqslant 20$, $2 < Z_2 < 10$, where for each fragmentation (A_1, A_2) the cross section is calculated in terms of its formation and penetration probabilities P_0 and P.

P_{surv}, determined for some 16 "hot" fusion reactions at various incident c.m. energies, covering the CN mass range of $A \sim 100$ to superheavy nuclei, is analyzed on DCM for various nuclear interaction potentials like the Blocki *et al.* pocket formula and the SEDF-based ones due to Skyrme SIII, SSk, and GSkI forces. Its variation with CN excitation energy E^*, fissility parameter χ, CN mass number A_{CN}, and Coulomb interaction parameter Z_1Z_2 is studied for both the in-plane (coplanar) and out-of-plane (noncoplanar) collisions. One of the interesting results is that the chosen 16 reactions fall in three groups of weakly fissioning, radioactive, and highly fissioning superheavy nuclei. For the weakly fissioning nuclei (of CN mass region $100 < A_{\mathrm{CN}} \lesssim 200$ with Coulomb interaction parameter of range $240 < Z_1Z_2 < 1400$), independent of the choice of nuclear interaction potential, different isotopes of the compound system, and their being coplanar or noncoplanar, $P_{\mathrm{surv}} \sim 1$ for lower E^* values and decreases from 1 to 0 as the excitation energy E^* increases. This happens due to the increasing ff component with increasing E^*. Exactly the same result is obtained for superheavy nuclei with $Z_1Z_2 \sim 1860 \pm 20$, except that, in agreement with experimental estimates [52], $P_{\mathrm{surv}} \sim 10^{-10}$ due to their being highly fissioning systems. On the other hand, for the third group of radioactive nuclei (of CN mass $A_{\mathrm{CN}} \sim 200$–250 with $410 < Z_1Z_2 < 632$), independent of entrance channel effects, P_{surv} has an intermediate value of $\sim 10^{-8}$–10^{-4} which, instead of decreasing, increases with increasing E^* due to the negligible small magnitude of (predicted) σ_{ER}, relative to (measured) σ_{ff}. Another interesting result is as follows: compared to ^{217}Fr*, ^{213}Fr* is more fissile (lower P_{surv}) and both ^{213,217}Fr* belong to the weakly fissioning group of nuclei with $P_{\mathrm{surv}} \sim 1$. On the other hand, independent of entrance channel, ^{215}Fr* is most fissile of all (lowest P_{surv}) that it belongs to the radioactive group of nuclei with $\sim 10^{-6}$. Note that though the fissility parameter χ for all the three isotopes ^{217,215,213}Fr* is nearly the same, the Z_1Z_2 for ^{213,217}Fr* is larger compared to that for ^{215}Fr*.

From a relative comparison of the variations of $P_{\rm CN}$ and $P_{\rm surv}$, we notice that whereas for Pt* isotopes both $P_{\rm CN}$ and $P_{\rm surv}$ decrease with the increase of E^*, for all the other compound systems considered here the variations of $P_{\rm CN}$ and $P_{\rm surv}$ with E^* are the reverse of each other, one increasing and the other decreasing. Similarly, for ^{105}Ag*, it belongs to the superheavy region for the $P_{\rm CN}$ value, but to weakly fissioning nuclei for $P_{\rm surv}$. This result should have important consequences for the product $P_{\rm CN} \times P_{\rm surv}$, and hence for the ER cross sections [refer to Eq. (3)].

Finally, it will be interesting to extend these calculations to more and more reactions, and also to "cold" fusion reactions to see if the above-noted results are kept the same or some new trends emerge.

ACKNOWLEDGMENTS

This work was supported in part by the Women Scientist scheme (WOS-A), Grant No. SR/WOS-A/PS-52/2013(G), Ministry of Science & Technology, Department of Science & Technology (DST), Government of India. A part of the computation for this work was performed at the in-house CAS-FIST-PURSE High Performance Computing Cluster (HPCC) Facility of the Department of Physics, Panjab University, Chandigarh (India).

[1] A. Kaur, S. Chopra, and R. K. Gupta, Phys. Rev. C **90**, 024619 (2014).

[2] S. Chopra, A. Kaur, and R. K. Gupta, Euro. Phys. J. Web Conf. **86**, 00006 (2015).

[3] R. Vandenbosch and J. R. Huizenga, *Nuclear Fission* (Academic, New York, 1973), p.323.

[4] W. Reisdorf, Z. Phys. A **300**, 227 (1981).

[5] A. V. Ignatyuk *et al.*, Sov. J. Nucl. Phys. **21**, 612 (1975).

[6] H. A. Kramers, Physica **7**, 284 (1940).

[7] R. K. Gupta, in *Clusters in Nuclei*, Lecture Notes in Physics 818, edited by C. Beck, Vol. I (Springer Verlag, Berlin, 2010), pp. 223–265; and earlier references there in.

[8] R. K. Gupta, M. Balasubramaniam, C. Mazzocchi, M. La Commara, and W. Scheid, Phys. Rev. C **65**, 024601 (2002).

[9] R. K. Gupta, R. Kumar, N. K. Dhiman, M. Balasubramaniam, W. Scheid, and C. Beck, Phys. Rev. C **68**, 014610 (2003).

[10] M. Balasubramaniam, R. Kumar, R. K. Gupta, C. Beck, and W. Scheid, J. Phys. G: Nucl. Part. Phys. **29**, 2703 (2003).

[11] M. Bansal and R. K. Gupta, Romanian J. Phys. **57**, 18 (2012).

[12] B. B. Singh, M. K. Sharma, R. K. Gupta, and W. Greiner, Int. J. Mod. Phys. E **15**, 699 (2006).

[13] B. B. Singh, M. K. Sharma, and R. K. Gupta, Phys. Rev. C **77**, 054613 (2008).

[14] S. K. Arun, R. Kumar, and R. K. Gupta, J. Phys. G: Nucl. Part. Phys. **36**, 085105 (2009).

[15] S. Kanwar, M. K. Sharma, B. B. Singh, R. K. Gupta, and W. Greiner, Int. J. Mod. Phys. E **18**, 1453 (2009).

[16] R. K. Gupta, Niyti, M. Manhas, S. Hofmann, and W. Greiner, Int. J. Mod. Phys. E **18**, 601 (2009).

[17] Niyti, R. K. Gupta, and W. Greiner, J. Phys. G: Nucl. Part. Phys. **37**, 115103 (2010).

[18] M. K. Sharma, S. Kanwar, G. Sawhney, R. K. Gupta, and W. Greiner, J. Phys. G: Nucl. Part. Phys. **38**, 055104 (2011).

[19] M. Bansal, S. Chopra, R. K. Gupta, R. Kumar, and M. K. Sharma, Phys. Rev. C **86**, 034604 (2012).

[20] D. Jain, R. Kumar, M. K. Sharma, and R. K. Gupta, Phys. Rev. C **85**, 024615 (2012).

[21] S. Chopra, M. Bansal, M. K. Sharma, and R. K. Gupta, Phys. Rev. C **88**, 014615 (2013).

[22] A. Kaur, S. Chopra, and R. K. Gupta, Phys. Rev. C **89**, 034602 (2014).

[23] M. K. Sharma, G. Sawhney, R. K. Gupta, and W. Griener, J. Phys. G **38**, 105101 (2011).

[24] M. K. Sharma, S. Kanwar, G. Sawhney, and R. K. Gupta, Phys. Rev. C **85**, 064602 (2012).

[25] G. Sawhney, G. Kaur, M. K. Sharma, and R. K. Gupta, Phys. Rev. C **88**, 034603 (2013).

[26] Niyti and R. K. Gupta, Phys. Rev. C **89**, 014603 (2014).

[27] A. Kaur, S. Chopra, and R. K. Gupta, Contribution 75 Years of Nuclear Fission: Present Status and Future Perspectives, May 8–10, 2014 at BARC, Mumbai; Book of Abstracts, p. 61.

[28] R. K. Gupta, M. Manhas, and W. Greiner, Phys. Rev. C **73**, 054307 (2006).

[29] R. K. Gupta, M. Balasubramaniam, R. Kumar, N. Singh, M. Manhas, and W. Greiner, J. Phys. G: Nucl. Part. Phys. **31**, 631 (2005).

[30] J. Maruhn and W. Greiner, Phys. Rev. Lett. **32**, 548 (1974).

[31] R. K. Gupta, W. Scheid, and W. Greiner, Phys. Rev. Lett. **35**, 353 (1975).

[32] D. R. Saroha and R. K. Gupta, J. Phys. G **12**, 1265 (1986).

[33] S. S. Malik, N. Malhotra, D. R. Saroha, and R. K. Gupta, ICTP, Trieste, Italy, Report No. IC/86/120, 1986.

[34] H. Kröger and W. Scheid, J. Phys. G **6**, L85 (1980).

[35] D. R. Inglis, Phys. Rev. **96**, 1059 (1954).

[36] S. T. Belyaev, K. Dan. Vidensk. Selsk. Mat. Fys. Medd. **31**, No. 11 (1959).

[37] N. J. Davidson, S. S. Hsiao, J. Markram, H. G. Miller, and Y. Tzeng, Nucl. Phys. A **570**, 61c (1994).

[38] G. Audi, A. H. Wapstra, and C. Thiboult, Nucl. Phys. A **729**, 337 (2003).

[39] W. Myers and W. J. Swiatecki, Nucl. Phys. **81**, 1 (1966).

[40] J. Blocki, J. Randrup, W. J. Swiatecki, and C. F. Tsang, Ann. Phys. (NY) **105**, 427 (1977).

[41] M. Brack, C. Guet, and H.-B. Hakansson, Phys. Rep. **123**, 275 (1985).

[42] J. Friedrich and P.-G. Reinhard, Phys. Rev. C **33**, 335 (1986).

[43] B. K. Agrawal, S. K. Dhiman, and R. Kumar, Phys. Rev. C **73**, 034319 (2006).

[44] W. Pauli, *Handbuck der Physik*, Vol. 24, Part I, p.120, edited by H. Geiger and K. Sheel (Springer, Berlin 1933); B. Padolsky, Phys. Rev. **32**, 812 (1928); J. Eisenberg and W. Greiner, *Nuclear Models* (North Holland, Amsterdam, 1971), p.136.

[45] R. K. Gupta, in *Proceedings of the 5th International Conference n Nuclear Reaction Mechanisms, Varenna, Italy*, edited by E. Gadioli (Ricerca Scientifica Educazione Permanente, Milan, Italy, 1988), p. 416.

[46] S. S. Malik and R. K. Gupta, Phys. Rev. C **39**, 1992 (1989).

[47] G. Royer and J. Mignen, J. Phys. G: Nucl. Part. Phys. **18**, 1781 (1992).

[48] H. S. Khosla, S. S. Malik, and R. K. Gupta, Nucl. Phys. A **513**, 115 (1990).
[49] S. Kumar and R. K. Gupta, Phys. Rev. C **55**, 218 (1997).
[50] R. K. Gupta, S. Kumar, and W. Scheid, Int. J. Mod. Phys. E **6**, 259 (1997).
[51] R. Kumar, M. Bansal, S. K. Arun, and R. K. Gupta, Phys. Rev. C **80**, 034618 (2009).
[52] E. M. Kozulin, G. N. Knyazheva, I. M. Itkis, M. G. Itkis, A. A. Bogachev, E. V. Chernysheva, L. Krupa, F. Hanappe, O. Dorvaux, L. Stuttgé, W. H. Trzaska, C. Schmitt, and G. Chubarian, Phys. Rev. C **90**, 054608 (2014).